

Spectrophotometric method for optimizing image capture conditions for inspecting protected documents

T. NECSOIU^a, G. BOSTAN^{a,b}, P. STERIAN^{b,c}

^aOptoelectronica-2001 SA, Bucharest, Romania.

^{a,b}University "Politehnica" of Bucharest, Academic Center for Optical Engineering and Photonics, Faculty of Applied Sciences, Physics Department, Romania

^cAcademy of Romanian Scientists, Splaiul Independentei No. 54, Bucharest 050094, Romania

The study presents a spectrophotometric system and method for the verification of documents based on the control of light sources and the correct lighting, to have a clear image. It points out the need to optimize optical schemes, measurements and estimates by additional means of illumination. It analyses the opportunity to use CMOS sensor of Digital Camera for spectrophotometric colour measurement in diffused reflection. The method of control of the reflection spectrum, proposed in the work will allow improving the device. For a document verification device, the spectrophotometric measurement function is very important, thus pursuing the integration of several functions in one device. Devices of colour reproduction appear more and more sophisticated hence the need to detect counterfeits by analysing ink by spectroscopic methods in addition to other verification methods is essential.

(Received September 26, 2017; accepted November 28, 2017)

Keywords: Optical security elements, Optical properties, Optical methods, Spectroscopic imaging

1. Introduction

A multitude of documents with varying degrees of protection can have different security levels, so that the complex protection features and visual features of the documents made by special technologies allow determining their authenticity in different applications [1, 2, 14].

The method of graphic protection involves a set of methods, based on graphical forms, size characteristics, and methods of arrangement and combination of elements of the graphical image. The graphical image can be visible or invisible under normal lighting conditions and visualized by ultraviolet (UV) and infrared (IR) rays. Data protection methods may include: the watermark; microtext; grid pattern; irregular raster; a variety of shapes and combination of fonts; the combination of various shape and form protective grid pattern (Fig. 1), specially made at the micro level defects of graphical elements; pseudo fibre; as well as other items [3-5].

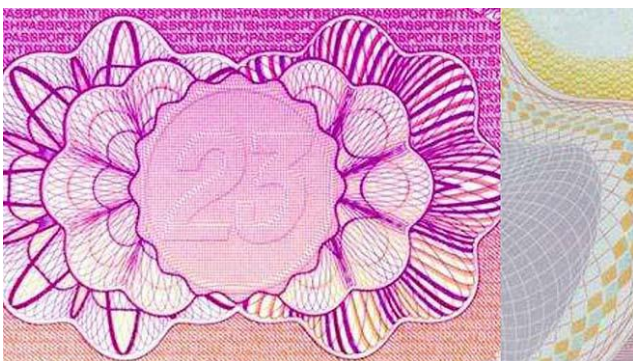


Fig. 1. Elements of fine-line patterns [4]

These methods refer to the totality of the optical security elements, the processes, which allow obtaining the concrete effect, observable visually or with the help of specialized equipment. In this respect there must be a clear distinction between the elements of protection for the user and for experts. For the user there are important elements allowing quick and simple identification without the use of special equipment, methods and conditions of observation. Watermarked paper is a good example for this. For expertise, in addition to visual characteristics, the confirmation of authenticity by special methods using special equipment is very important.

To effectively solve the problem of detecting fakes and forgeries special opto-electronic systems, video comparators can be used. A video comparator is an optical tool for introscopy, and non-destructive testing of document surfaces by using optical control methods in reflected and transmitted light in a wide spectrum of wavelengths. It ensures the authenticity of document detection and allows recording fingerprints and other traces of intervention

In addition to the use of UV radiation, the use of high efficiency blue light (470 nm) and green light (520 nm) ensures high optical contrast at the luminance of the specific protection elements.

The range of emission from yellow-green (550 nm) and yellow (580 nm) to red (650 nm) can detect labels, and stamps, destroyed by chemical etching, to restore the image of the stamps or primary labels, filled with ink to identify the notes and corrections of texts.

Under illumination by infrared radiation, for example, the luminescence of special elements in the visible range can be observed.

Checking the whole set of protective elements may confirm the authenticity of the document.

Discussing about methods of securing documents we consider technological protection, physical-chemical and printing. Technological protection is implemented in the substrate of the document, which generally is paper.

By briefly analysing the optical properties and optical methods of inspection of documents for detecting counterfeits, in the results we discuss the device diagram for verification of documents, considering the possibility of broadening the functionality, optimization of light sources, efficient use of CMOS camera, having studied the quality of the recorded images. At the end of the article we shall put down the conclusions.

2. Optical methods of document control

Spectroscopic imaging is a powerful tool to visualize the objects and their properties because almost all optic material constants such as the reflectivity, the index of refraction, the absorption coefficient, the scattering coefficient and luminescence depend on the wavelength of the radiation. Spectral lighting adds another coordinate to imaging and the required amount of data is multiplied correspondingly. Therefore, it is important to sample the spectrum with a minimum number of samples that is sufficient to perform the required task.

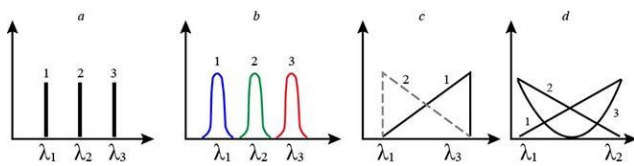


Fig. 2 Examples for spectral sampling: a) line-sampling, b) band-sampling, c) sampling to measure the total radiative flux and the mean wavelength, d) sampling to measure the total radiative flux, the mean wavelength and the variance of the wavelength [6]

a) Line sampling, this technique is useful if the processes to be imaged are related to emission or absorption at specific spectral lines.

b) Band sampling, we can measure the spectral radiance with a resolution given by the width of the spectral bands.

c) In many cases, it is possible to make a model of the spectral radiance of a certain object. Then, a much better spectral sampling technique can be chosen that essentially does not sample certain wavelengths but rather the parameters of the model [6-10]. To measure the mean wavelength of an arbitrary spectral distribution $H(\lambda)$ ("colour") and the total radiative flux ("intensity") in a certain wave number range, the quantities are defined as [6]:

$$\Phi = \frac{1}{\lambda_2 - \lambda_1} \int_{\lambda_1}^{\lambda_2} \Phi(\lambda) d\lambda, \quad \bar{\lambda} = \frac{\int_{\lambda_1}^{\lambda_2} \lambda \Phi(\lambda) d\lambda}{\int_{\lambda_1}^{\lambda_2} \Phi(\lambda) d\lambda} \quad (1)$$

$$R_1(\lambda) = \frac{\lambda - \lambda_1}{\lambda_2 - \lambda_1} R_0 = \left(\frac{1}{2} + \tilde{\lambda}\right) R_0 \quad (2)$$

$$R_2(\lambda) = R_0 - R_1(\lambda) = \left(\frac{1}{2} - \tilde{\lambda}\right) R_0,$$

R_1, R_2 are the responsivity of the sensors, given as $R=s/\Phi$ (units A/W), s the sensor signal, usually given in units for the electronic current, and $\tilde{\lambda}$ the normalized wavelength

$$\tilde{\lambda} = \left(\lambda - \frac{\lambda_1 + \lambda_2}{2}\right) / (\lambda_2 - \lambda_1) \quad (3)$$

$\tilde{\lambda}$ is zero in the middle of the interval and $\pm 1/2$ at the edges of the interval. The sum of the responsivity of the two channels is wavelength independent, while the difference is directly proportional to the wavelength and varies from -1 for $\lambda = \lambda_1$ to 1 for $\lambda = \lambda_2$.

d) Measurement of Chemical Species by Imaging Spectroscopy. The absorption of various chemical species differs significantly and thus can be used to identify them and to measure their concentration, the surface receiving different amounts of light from different illumination directions and may radiate different amounts of light in different outgoing directions.

An imaging system collects the radiation emitted by objects to make them visible. In classical computer vision, scenes and illumination are taken and analysed as they are given, but visual systems used in scientific and industrial applications require a different approach. There, the first task is to establish the quantitative relation between the object feature of interest and the emitted radiation [6].

Surface reflectance and illumination power spectrum are wavelength dependent. The imaging process is concerned with the distribution of light in space as a function of position and direction. The most general model of local reflection is the bidirectional reflectance distribution function (BRDF). Reflection geometry is defined with respect to a right handed local coordinate system, whose origin is the surface location under examination, and z -axis aligns with the local normal surface (Fig. 3). In this coordinate system, the illuminant and viewing directions are described by two pairs of angles (θ_i, φ_i) and (θ_r, φ_r) , where θ_i and θ_r are the zenith angles and φ_i and φ_r are the azimuth angles of the respective directions. The solid angle of the cone of incident light rays when viewed from the surface is annotated as $d\omega_i$ in Fig. 3. We assume that the source radiance $L(\lambda)$ with wavelength λ is almost constant across all the incoming directions.

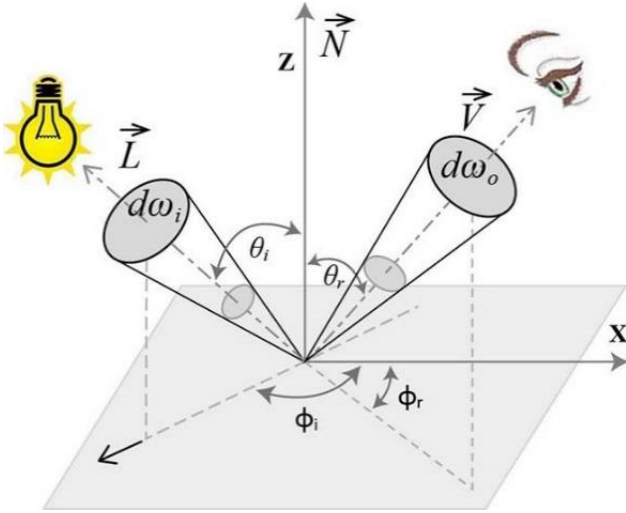


Fig. 3 The BRDF $f(\theta_i, \phi_i, \theta_r, \phi_r, \lambda)$ quantifies the fraction of incident light that is reflected from the surface into the air in various directions, X is referention direction. The source irradiance, the surface radiance and the BRDF depend on the wavelength λ [11]

Thus, the energy flux per unit area perpendicular to the light direction is proportional to the source radiance and the solid angle, i.e. $L(\lambda) d\omega_i$. Due to the foreshortening effect, the irradiance $E_i(\theta_i, \phi_i, \lambda)$ arriving at the surface is, however, measured per unit area perpendicular to the local surface normal,

$$E_i(\theta_i, \phi_i, \lambda) = L(\lambda) \cos \theta_i d\omega_i, \quad (4)$$

The mathematical model presented is important to understand the linear optical phenomena (reflection, refraction, diffusion) produced by light at the interface of two media, in the simplified model of geometric optics. Light propagates in a three-dimensional space. Having a fixed light source, we observe different reflections from fixed area when changing the position of the observer. Having fixed the observer and changing the position of the light source will also see different reflections from the same fixed area, so sometimes do not understand each other because we see differently, not in this case. Therefore, this simple refinement at a first glance is important for computer vision.

Let the light source energy arriving at the surface in the direction (θ_i, ϕ_i) be $E_i(\theta_i, \phi_i, \lambda)$, and the radiance at the same surface point, seen from the direction (θ_r, ϕ_r) be $E_o(\theta_i, \phi_i, \theta_r, \phi_r, \lambda)$. The BRDF of the surface is the ratio of the outgoing radiance to the incoming irradiance,

$$f(\theta_i, \phi_i, \theta_r, \phi_r, \lambda) = \frac{E_o(\theta_i, \phi_i, \theta_r, \phi_r, \lambda)}{E_i(\theta_i, \phi_i, \lambda)} \quad (5)$$

Note that the source irradiance, the surface radiance and the BRDF are dependent on the wavelength λ , E_o being outgoing radiance. From equations (4) and (5) yields the surface radiance:

$$E_o(\theta_i, \phi_i, \theta_r, \phi_r, \lambda) = f(\theta_i, \phi_i, \theta_r, \phi_r, \lambda) L(\lambda) \cos \theta_i d\omega_i \quad (6)$$

We admit that the flux radiated from the surface is transmitted through the camera lens without any loss of energy. The irradiance reaching the image plane is given by [11]

$$I_{im}(\lambda) = \frac{\pi}{4} \left(\frac{d}{z}\right)^2 \cos^4 \alpha E_o(\theta_i, \phi_i, \theta_r, \phi_r, \lambda) = mf(\theta_i, \phi_i, \theta_r, \phi_r, \lambda) L(\lambda) \cos \theta_i \cos^4 \alpha d\omega_i \quad (7)$$

where d is the lens diameter, z is the distance between the lens and the image plane, $m \triangleq \frac{\pi}{4} \left(\frac{d}{z}\right)^2$ and α is the angle between the optical axis of the camera and the line of sight from the surface patch to the centre of the lens. The term m depends on the camera geometry [11-13,15].

Consider the relationship between trichromatic imagery and imaging spectroscopy data, a general formulation for a particular colour channel c , where $c \in \{R, G, B\}$, the spectral sensitivity functions, i.e. the colour matching functions, of the red (R), green (G) and blue (B) sensors be denoted $C_R(\lambda)$, $C_G(\lambda)$ and $C_B(\lambda)$, respectively, the response for the colour sensor is given by [11]

$$I_c = k_c \int_W C_c(\lambda) I_{im}(\lambda) d\lambda = m k_c \cos \theta_i \cos^4 \alpha d\omega_i \times \int_W C_c(\lambda) f(\theta_i, \phi_i, \theta_r, \phi_r, \lambda) L(\lambda) d\lambda \quad (8)$$

where $W=[380 \text{ nm} \dots 780 \text{ nm}]$; in eq. (8) the value of k_c corresponds to the colour balance factor of the camera against a predetermined reference. By colour balancing, the values of I_B , I_G and I_R are scaled such that a smooth surface, with BRDF $f(\theta_i, \phi_i, \theta_r, \phi_r, \lambda)=1$, placed perpendicularly to the camera axis. The diffuse reflection effect at large incident and viewing angles was observed on many dielectric objects. The model was derived from the theory of radiative transfer through boundaries between dielectric layers. Formally the diffuse reflectance formulated by the Wolff model (1994) is given by [11, 22]

$$f_W(u, \lambda) = \rho(u, \lambda) \cos \theta_i \left(1 - F(\theta_i, \eta(u, \lambda))\right) \times \left(1 - F\left(\theta'_s, \frac{1}{n(u, \lambda)}\right)\right), \quad (9)$$

where $\rho(u, \lambda)$ is the total diffuse albedo accumulated by multiple diffuse subsurface scattering, $n(u, \lambda)$ is the index of refraction of the dielectric medium and θ'_s is the internal angle of incidence on the dielectric-air boundary before the light ray is refracted and re-emerges from the surface. The Wolff model consists of Lambert's cosine term multiplied by two Fresnel transmission terms. The $\cos \theta_i$ factor is borrowed from the Lambertian model to account for foreshortening of the incident ray viewed from the point of incidence on the surface. In addition, the Fresnel term $\left(1 - F\left(\theta'_s, \frac{1}{n(u, \lambda)}\right)\right)$ accounts for the refraction of the emitted light ray [11].

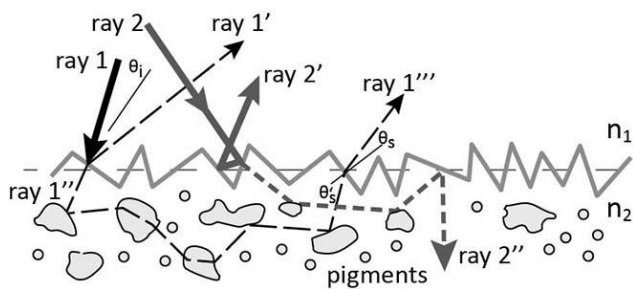


Fig. 4. Reflected and refracted light components [12]

When light interacts with a rough surface, we can observe several optical phenomena, refraction, reflection, scattering, and absorption, when light (ray 1 and ray 2) Fig. 4, are incident on the rough surface, part of its energy is reflected (ray 1' and ray 2') and part of it penetrates into the surface (ray 1'' and ray 2''). The reflected light can undergo more than one reflection (ray 2'). The penetrating light can undergo multiple scattering by pigment particles in the surface material, and eventually is absorbed (ray 2'') or reflected back into the air (ray 1'''). The first reflection at the interface (ray 1' and ray 2') has several names: surface reflection, interface reflection, or specular reflection. Reflection coming from under surface (ray 1''') also has several names: subsurface reflection, body reflection, bulk reflection, or diffuse reflection. Strictly speaking, there are problems with all these names and they come from the very basic fact that light cannot be treated as being reflected only at the interface, but rather the incident light interacts with all atoms and molecules in the object [11, 12,18-21].

Machine Vision cameras and the human eye have different spectral perceptions of light (Fig. 5). The spectral response of the human eye covers the range of light between 380 nm and 780 nm and is described by the so-called $V(\lambda)$ curve (for daylight perception).

This curve is the base for the calculation of all photometric units such as luminous intensity, luminous flux and so forth. The light perception of Machine Vision cameras differs from the human eye. Machine Vision uses in most cases light with wavelengths between 380 nm and 1100 nm (from blue light to near infrared). This is caused by the reception and spectral response of the imagers. The data sheet of the image sensor used in the camera informs about this.

Machine Vision illumination components for industrial use are complex technical systems consisting of light sources, mechanical adjustment elements, light guiding optical elements, stabilizing, controlling and interface electronics, and if necessary software (firmware), stable and mountable housing, robust cabling.

All these features are necessary to form a device that resists the adverse environmental conditions of the industrial floor [14].

The possibility of expanding the device functionality at the same time with the emergence of new theories and technologies must be also permanently investigated [11, 22-25].

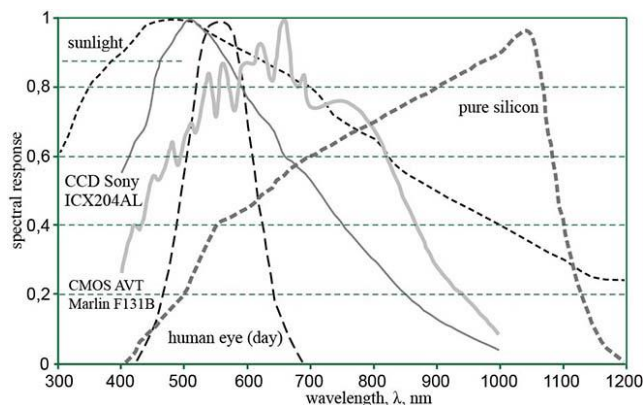


Fig. 5. Spectral response of the human eye, typical monochrome CCD image sensor (Sony ICX204AL), typical monochrome CMOS image sensor (camera AVT Marlin F131B), the spectral emission of the sun [15]

3. Operating principles and technical aspects

The device is designed for checking identity documents, and other documents with protective elements. It has an enclosure in which it is placed face up, document examined.

From the distance of approx. 24cm is situated the CMOS camera that displays on the computer screen the document image in real time. The camera can zoom into different parts of the document to examine areas of interest. Chamber of the device has a complex lighting system that helps the camera to view areas of interest on the surface of the document. It has several light sources for various types of lighting which differentiates it by the emission spectrum: visible, ultraviolet, infrared. Against certain bulbs are placed optical band filters to highlight various aspects of the document image.

The spectral characteristic of bulbs ensure the efficient lighting of the document that contains elements of different colours; b) by the type of lighting, oblique, coaxial, transmission. The reflection from paper of document is diffuse. For plastic laminated documents, lacquered with glossy surfaces different angle of illumination is selected, to obtain better diffuse reflectance. In the case of highly reflective metallic elements, polarized lighting is recommended, so that the rays that give shine to be rejected and reflections in scattered light to be accepted. The appliance is equipped with special software that processes the acquired images recorded by the camera. In front of the camera lens there are located two turrets with optical filters, used to filter reflections from areas of the document under examination. The combination of optical filters can be: passing down, high pass, band pass, for different spectral ranges. Some of the filters can be removed from the optical scheme, replacing the current lamps with LEDs with necessary emission spectrum. The lighting system is equipped with UV (ultraviolet) lamps for viewing fluorescent fibre protection, inserted in the paper of the document. The document to be examined is placed on a matte glass plate

which has lighting bulbs underneath, lighting by transmission for semi-transparent sheets

Camera lens must have a sufficient optical zoom to view the Microprint, $0.1 \div 0.2$ mm, a technical problem that requires optimization, by finding solutions to technological upgrade; the lighting scheme is controlled by computer software. The optical system of the device is presented in Fig. 6.

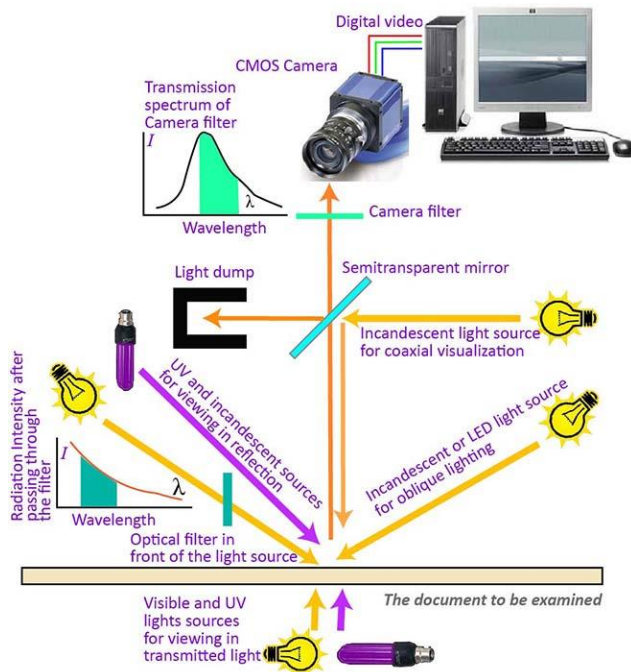


Fig. 6. Device schema for document authenticity verification

The device is composed of a camera with 5 megapixel CMOS sensors, connected to the PC, containing various light sources that provide illumination efficiency, bandwidth optical filters.

At the same time with the evolution of technology, a new feature of the device is implemented: spectroscopic analysis of ink signatures and stamps. Some equipment manufacturers show the technical specifications of the machine, a new function for colorimetric measurements using the CMOS camera and linear interference filter placed in front of the camera.

The CMOS camera sensor uses the Bayer demosaicing algorithm, for interpolation and processing recorded image, does not provide authentic data about the colour, as shown in Fig. 7. To understand the functioning, it is necessary to remember how colours are recorded by the optical sensor with Bayer filter aid [16, 21].

Bayer demosaicing is a transfer algorithm of Bayer matrix, containing data on the three RGB primary colours in the final image with complete data on colour for each pixel separately [11]. Let us examine a matrix of 2×2 pixels as a single pixel full colour (Fig. 7, pixel 5). If the camera treated a 2×2 pixel arrays as a single pixel full colour, the sensor resolution would halve, both horizontally and vertically. The camera calculates the colour using the overlapping matrices, so the image

resolution increases, compared to the 2×2 matrices which are presented as a single pixel full colour. Image pixels 5 are obtained by grouping the 2×2 sensor pixels, big pixel 5 has the two pixels from the left side, Green and Blue, which have been used for the colour formation of pixel 1. This algorithm is applied not to lose image resolution, to use with maximum efficiency optical sensor pixels. This algorithm works perfectly, so additional steps are made to extract more information about colour from matrix filters.

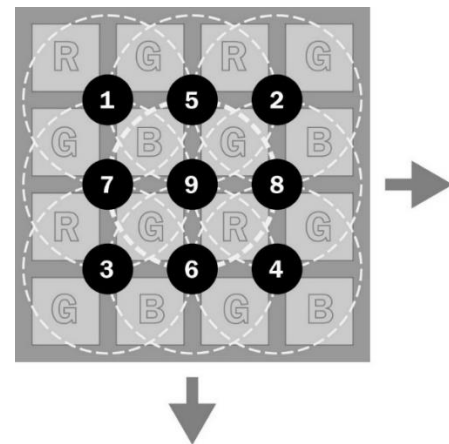


Fig. 7. Bayer demosaicing algorithm. Image pixels (1; 5; 2; 7; 9; 8; 3; 6; 4) in the above chart, are no longer sensor pixels, are pixels of a picture produced by the sensor processor. In this situation the colour information is synthesised by the sensor processor

Fig. 7 shows how the algorithm grouped sensor pixels to form final image, without losing resolution, but losing the initial data about colour for each pixel. It should be noted, there are other algorithms of processing, which produce images with low noises, and a better approximation of the image.

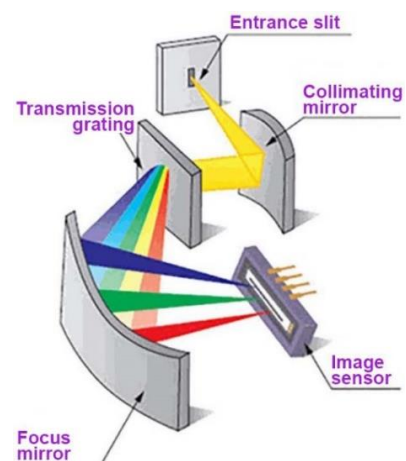


Fig. 8. Linear optical sensor array for spectrometry [16]

The interpolation algorithm producing colour pixel based on colour information from neighbouring pixels, the camera sensor cannot serve as a colorimeter or spectrophotometer. Firstly, manufacturers of optical sensors for

commercial cameras do not say anything about this function.

Sensors for spectrometers are linear arrays of photosensitive pixels, connected in a well-aligned optical scheme, did not have to face the Bayer filter. On the photosensitive cells falls monochromatic light (Fig. 8). Unlike the photo camera, the spectrometer decomposes ray light into monochromatic light that is reflected from the area analysed.

4. Results

4.1. Experimental data the spectral characteristics

Low quality images are the result of the lighting sources with improper emission spectrum. The spectrum of lighting source should contain spectral components that will be better reflected from foreground items on the document to be examined, and much less from the background. A document fragment of low contrast, which contains micro printing 0.1 mm, recorded with a CMOS camera (Fig. 12), is presented for examination.

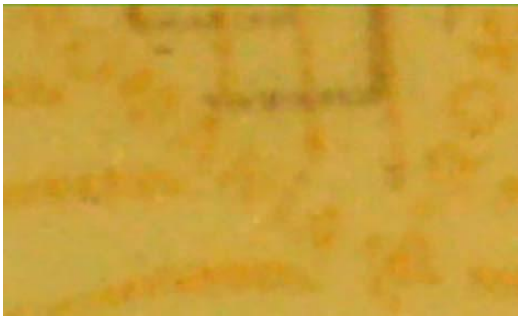


Fig. 9. Low contrast image

The document contains elements that are difficult to view, because they are on a background that has shades of close colours. As a result, low contrast and sharpness image are deteriorated due to incident light scattering in the paper fibrous substrate, which in some adverse conditions may increase the loss of contrast (Fig. 9).

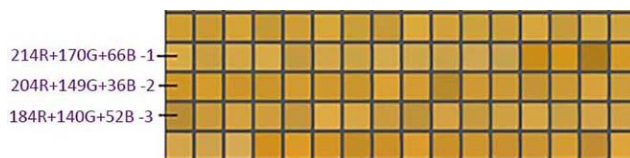


Fig. 10. Part of the colour palette of the low contrast image presented in Fig. 12

Some radiation from the emission spectrum of the light source can interact with the background, generating a weak luminescence of the fibres of the paper substrate, multiple internal reflections in the paper substrate medium [16,17] in printing pigments and other effects of light scattering.

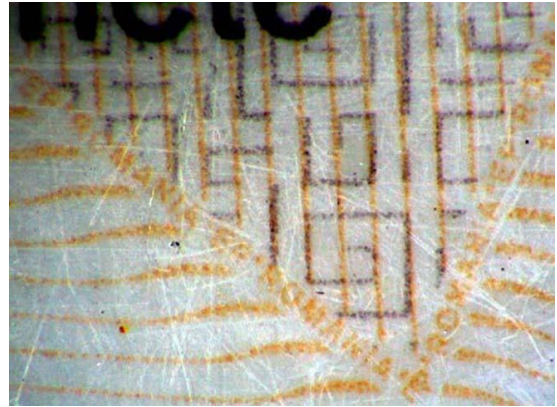


Fig. 11. Lighting conditions modified for Fig 9

Before talking about the quality of the camera lens, the optical resolution, we analyse the phenomenon of how substrate colour is changed depending on the change in emission spectrum of the lamp (Fig. 11).

For the estimation of influence, it is necessary to modify optical band of radiation source with the pass filters and watch under a microscope, image quality for each optical filter. It is important to have adjustments for the angle of incidence of the light flow. The image exhibited in Figure 9 has a very narrow palette of colours (small differences between shades). Figure 10 shows a part of the colour palette of the image.

For example colours 1, 2 and 3 are very close to the human eye, but have different RGB components. To achieve a good contrast it is necessary to have adequate lighting. To select the correct light source, you need to estimate the reflection spectrum of the surface to be examined. Fig. 12 shows the emission spectrum from an orange region of the document.

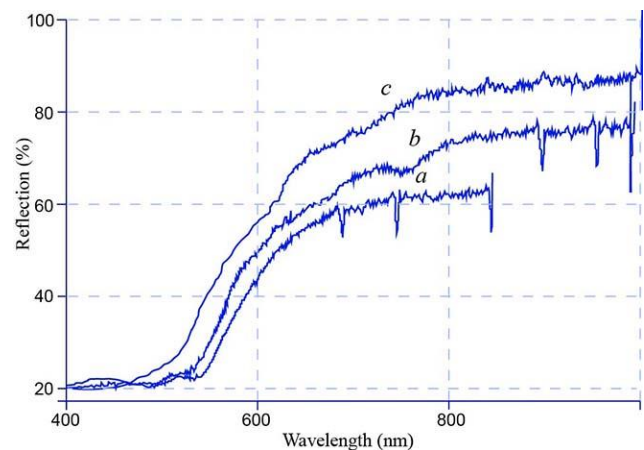


Fig. 12. The reflection spectrum of orange pigment (Ocean QE65000 spectrometer)

In the spectral region of 600 nm, there is an increase in reflection for the orange colour tone. In order to have a good reflection, it is necessary that the light source contain the spectral components that are very well reflected by the polygraphic pigments analysed. Curves a, b and c show

that reflection depends on both surface roughness and the angle of incidence of light rays. The document in the apparatus is fixed manually, at the slightest movement of the sample it will produce a redistribution of reflected spectral components. Bidirectional reflectance distribution function BRDF expresses these changes very well (2.5)

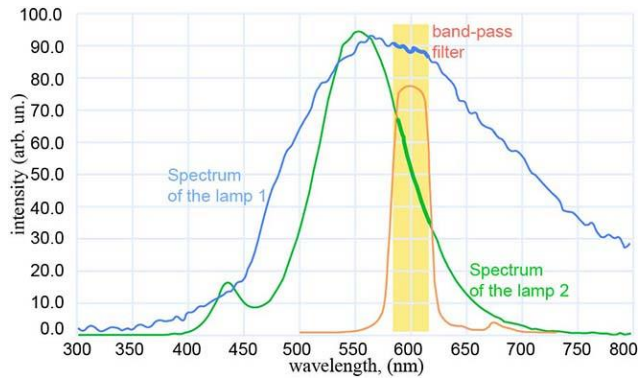


Fig. 13. Spectrum of the optical band filter overlaid over the spectra of light sources 1 and 2 in the 600 nm region illustrates how the device selects the wavelengths (registered by the Ocean QE65000 spectrometer)

The emission spectra of light sources and optical band pass filters was registered to estimate optimum lighting conditions

The incident light spectrum on the sensor is the superposition of light source emission, document surface reflection, camera spectral sensitivity spectra (Fig. 14).

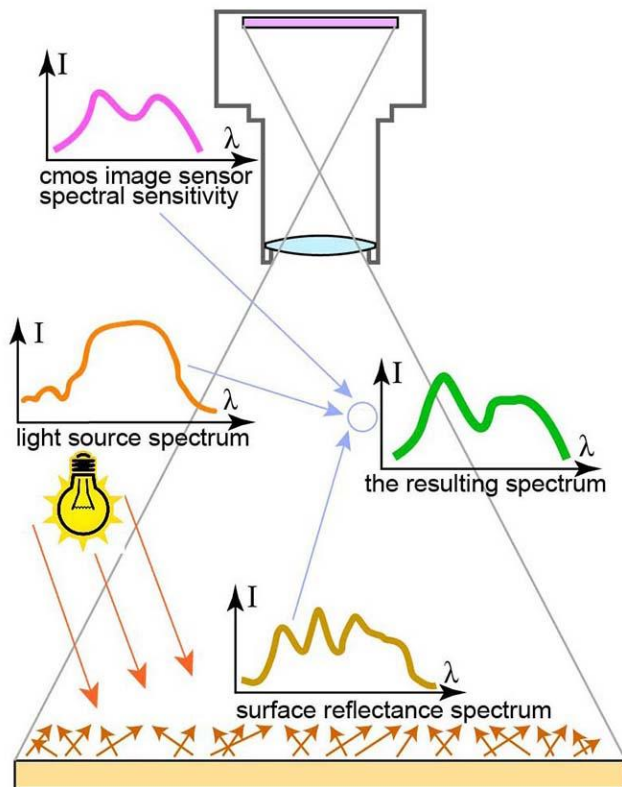


Fig. 14. The superposition of the spectral characteristics

The pass band filters will be placed in front of the light source, not in front of the camera, to remove those spectral components that can induce unwanted optical effects, such as diffusion or luminiscence on the surface under examination. The image in Fig. 9 has been recorded with high-performance camera, but due to inadequate illumination it has a low contrast. By manipulating the source emission spectrum of light we can control the reflection and image quality. To increase the contrast of the recorded images we need a proper selection of lighting sources.

4.2. Matrix representations and calculations

The spectral curves were calculated using the Matlab multi-paradigm numerical computing environment from MathWorks, Inc and Microsoft Excel spreadsheet programme, a grid interface to organise scientific data and formulas, to perform calculations. We would like to express our gratitude to the creators of these wonderful work tools.

Spectral data as continuous functions of wavelength are convenient to represent as vectors and matrices. Matrix algebra greatly simplifies the implementation of machine vision algorithm. Discrete representation causes the information loss but sampling can be made arbitrarily small by sampling at smaller intervals. In photometric and colorimetric applications, sample wavelengths are typically spaced evenly throughout the visible spectrum at steps of 1, 5, or 10 nm or more. Intensity scaling is an operation that changes the overall power of a light at each wavelength without altering the relative power between any pair of wavelengths.

Illuminants and surfaces are of interest in machine vision applications involving inks, paints, dyes, lighting design applications. We will use the vector e (lowercase bold italic letters) to represent illuminant spectral power distributions. The interaction of light with matter is quite complex. For many applications, however, a rather simple model is acceptable. The surface reflectance function specifies, for each sample wavelength, the fraction of illuminant power that is reflected to the observer. We shall use the vector s to represent surface reflectance spectra. Each entry of s gives the reflectance measured at a single sample wavelength. Thus the spectral power distribution b of the reflected light is given by the wavelength product of the illuminant spectral power distribution and the surface reflectance function.

If a light b_1 is scaled by a factor k , then the result b is given by the equation

$$b = b_1 k$$

$$\begin{bmatrix} \cdot \\ \cdot \\ \cdot \\ b \\ \cdot \\ \cdot \\ \cdot \end{bmatrix} = \begin{bmatrix} \cdot \\ \cdot \\ \cdot \\ b_1 \\ \cdot \\ \cdot \\ \cdot \end{bmatrix} \cdot 0.3 \quad (10)$$

The relation between the surface reflectance function s and the reflected light spectral power distribution (SPD)

vector b is linear if the illuminant SPD is held fixed. The illuminant matrix E of size $n\lambda$ by $n\lambda$ are the entries of e . This is represented by the relation:

$$b = Es \tag{11}$$

The relation between the radiant power emitted by the source of illumination, the material properties of a surface, and the radiant power reaching an observer (or CMOS sensor) can depend strongly on the viewing geometry, so that any actual calculation is specific to a particular viewing geometry (Fig. 3).

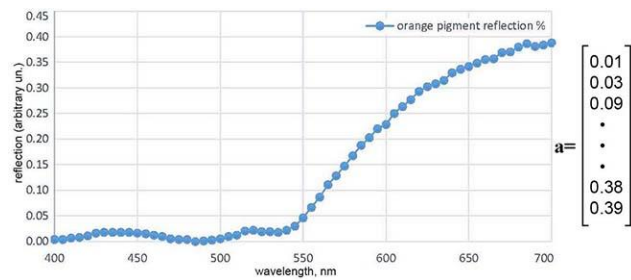


Fig. 15. Reflectance spectra of orange pigment as vector

Reflectance spectra of orange pigment is measured with 5 nm step over the range 400-700 nm. The points on the graph are the reflection for each wavelength (vector a). The vector a on the right represents the same data in a matrix form. The n th entry of a is simply the measured power density at the n th sample wavelength times $\Delta\lambda$. Thus a_1 is derived from the power density at 400 nm, a_2 is derived from the power density at 405 nm, and a_{61} is derived from the power density at 700 nm.

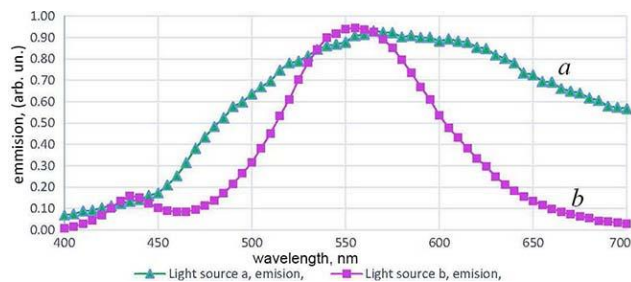


Fig. 16 The emission spectrum of two light sources, a-tungsten-lamp and b-LED. The spectral data was registered as vectors a and b

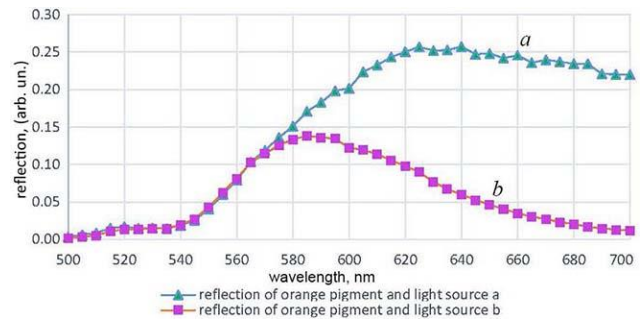


Fig. 17. Reflectance spectra of lamp a and lamp b reflected from orange pigment illustrated in (Fig. 16), the maximum reflectance shifted from 550 nm to 590 nm

5. Conclusions

The article discusses some optical characterisation methods of the protective elements of security documents and presents some results of the measurements performed.

From the recorded test images, it results that the type of lighting is very important for getting a clarity image, especially if the examining element has colour shades close to those of the background. The presented results will help to optimize the operation of the equipment, the widening capacity to distinguish close shades of colour. The method of control of the reflection spectrum proposed in the work will allow improving the device.

The exploration ways to highlight the microtext from the background, that almost blends in certain specific lighting conditions, before processing with the help of specialized software are necessary, because the optical system must record images of sufficient quality to prevent the spectra that are seen by the human eye as being different but which can be seen by the video camera and displayed as identical or nearly identical.

References

- [1] R. L. v. Renesse, A Review of Holograms and other Microstructures as Security Features, The Hague, The Netherlands: Formerly with TNO Institute of Applied Physics. Delft, the Netherlands, 2002.
- [2] C. C. P. Peter Bamfield, The Technological Application of Colour Chemistry, The Royal Society of Chemistry, 2001.
- [3] D. Savastru, S. Miclos, N. Iftimia, M. A. Calin, R. Savastru, D. Manea, S. Dontu, J. Optoelectron. Adv. M. **18**(11-12), 993 (2016).
- [4] PRADO Glossary Technical terms related to security features and to security documents in general, Council of the European Union General Secretariat, 2015.
- [5] B. Lazar, et al., Computational Science And Its Applications - ICCSA 2006, PT 1 Book Series: Lecture Notes Ln Computer Science **3980**, 779 (2006).

- [6] B. Jahne, Image Processing for Scientific and Technical Application, 2nd ed., University of Heidelberg: CRC Press, 2004.
- [7] Florina S. Iliescu, et al., University Politehnica of Bucharest Scientific Bulletin-Series A-Applied Mathematics And Physics **71**(4), 21 (2009).
- [8] Ioan Dancus, Silviu T. Popescu, Adrian Petris, Optics Express **21**(25), 31303 (2013).
- [9] D. Savastru, S. Miclos, S. Dontu, G. Inceu, C. Bondor, Optoelectron. Adv. Mat. **10**(11-12), 893 (2016).
- [10] A. R. Sterian, Computational Science and Its Applications - ICCSA 2007, Pt 1, Proceedings Book Series: Lecture Notes Ln Computer Science **4705**, 436 (2007).
- [11] C. P. H. Antonio Robles-Kelly, Imaging Spectroscopy for Scene Analysis, London: Springer-Verlag (2013).
- [12] H.-C. Lee, Introduction to Color Imaging Science, New York: Cambridge University Press, 2005.
- [13] C. Spulber, et al, 13th International School on Quantum Electronics, Bourgas, Bulgaria Sep 20-24,2004; Book Series: Proceedings of The Society of Photo-Optical Instrumentation Engineers (SPIE); **5830**, 434 (2005).
- [14] M. Dima, M. Dulea, D. Aranghel, et al, Optoelectron. Adv. Mat. **4**(11), 1840 (2010).
- [15] A. Hornberg, Handbook of Machine Vision, Weinheim: WILEY-VCH Verlag GmbH & Co KgaA, 2006.
- [16] Hamamatsu, "CMOS sensors for spectroscopy and industrial applications," [Online]. Available: https://www.hamamatsu.com/us/en/community/optical_sensors/articles/cmos_sensors_spectroscopy_industrial/index.html
- [17] A. R. Sterian, P. E. Sterian, Mathematical Problems in Engineering, **2012**, Article ID 347674, doi:10.1155/2012/347674, p. 12 (2012).
- [18] Constantin Rosu, et al., Modern Physics Letters B **24**(1), 65 (2010).
- [19] A. A. Popescu, R. Savastru, D. Savastru, et al., Digest Journal of Nanomaterials and Biostructures, **6**(3), 1245 (2011).
- [20] D. Manaila-Maximean, C. Rosu, Molecular Crystals and Liquid Crystals **413**(1), 9 (2004).
- [21] D. A. Kerr, "Colorimetric characterization of digital camera sensors," 18 10 2015. [Online]. Available: http://dougkerr.net/Pumpkin/#Colorimetric_Characterization.
- [22] L. B. Wolff, Journal of the Optical Society of America **11**(11), 2956 (1994).
- [23] E. Stefanescu, et al., Proc. SPIE 5850, Advanced Laser Technologies **2004**, 160 (2005). doi:10.1117/12.633686.
- [24] M. Zoran, R. Savastru, D. Savastru, et al., J. Optoelectron. Adv. M. **12**(1), 159 (2010).
- [25] A. Zaharia, V. Ciupinã, G. Prodan, A. Caraiane, J. Optoelectron. Adv. M. **17**(3-4), 323 (2015).

*Corresponding author: georgebostan@gmail.com